CSIRO PUBLISHING

Functional Plant Biology, 2014, **41**, 648–658
http://dx.doi.org/10.1071/FP13235

Stomatal pore size and density in mangrove leaves and artificial leaves: effects on leaf water isotopic enrichment during transpiration

Leonel da Silveira Lobo Sternberg[A,B] *and Lynn M. Manganiello*[A]

[A]Department of Biology, University of Miami, 1301 Memorial Drive, Coral Gables, FL 33146, USA.
[B]Corresponding author. Email: leo@bio.miami.edu

Abstract. We tested the hypothesis that the previously observed low isotopic enrichment of mangrove leaf water is caused by larger stomatal pores and lower densities compared with freshwater plants. First, we measured and compared pore size and density in mangroves, transitional and freshwater species in South Florida. We pooled this data with other reports encompassing 14 mangrove species and 134 freshwater species and tested for differences in pore size and density between mangroves and freshwater plants. Second, we built artificial leaves having different pore size and density and determined whether there were isotopic differences in their water after transpiration. Both the local survey and pooled data showed that mangrove leaves have significantly larger stomatal pores with lower densities compared with freshwater plants. Isotope enrichment of water from artificial leaves having larger less dense pores was lower than those having smaller and denser pores. Stomatal pore size and density has an effect on leaf water isotopic enrichment amongst other factors. Pore size and density probably affects key components of the Peclet ratio such as the distance advective flow of water must travel to the evaporative surface and the cross-sectional area of advective flow. These components, in turn, affect leaf water isotopic enrichment. Results from the artificial leaf experiment also mimic a recent finding that effective path length scales to the inverse of transpiration in real leaves. The implications of these findings further our understanding of leaf water isotope ratios and are important in applications of stable isotopes in the study of paleoclimate and atmospheric processes.

Additional keywords: hydrogen isotope ratios, leaf water, oxygen isotope ratios, paleoclimate, stomatal density, stomatal size.

Received 6 August 2013, accepted 20 December 2013, published online 29 January 2014

Introduction

Salinity imposes two types of stresses in terrestrial plants: first, by osmosis it causes plants to become water stressed just as in arid environments; and second, it causes toxicity to its metabolic apparatus, as the high ionic strength of salts will cause enzyme inactivation (Flowers *et al*. 1977; Flowers and Colmer 2008; Krauss and Ball 2013). In addition, roots of several mangrove and coastal marsh species grow and function under anaerobic conditions (Colmer and Flowers 2008). Mangroves and other halophyte plants have evolved several adaptations to these stresses. For example: *Rhizophora mangle* L. and other mangrove species have the ability of 'ultra-filtrating' salts away during water uptake by roots (Scholander 1968). Other mangrove species, such as *Avicennia marina* (Forsk.) have salt excreting glands at the surface of their leaves (Scholander *et al*. 1962). Succulence is another adaptation that allows for the storage of salts in large vacuoles (Flowers *et al*. 1977). An increase in water use efficiency (WUE) during the photosynthetic process, which is related to the stomatal behaviour of the plant (Farquhar *et al*. 1982), and even shifts in the photosynthetic pathway taken by the plant (Winter and Holtum 2005), are additional adaptations to salinity.

Many of the above adaptations will leave an isotope imprint in the plants natural isotope abundance, as it involves a difference in the carbon and water management by halophyte plants compared with freshwater plants. For example, the shift in the metabolic pathway from a C_3 pathway to a water conserving photosynthetic mode, known as crassulacean acid metabolism (CAM), under higher salinity has been recorded in the carbon isotope ratios of *Mesembryanthum crystalinum* L. (Winter and Holtum 2005). Increase in WUE with an increase in salinity, even without a shift in the photosynthetic pathway, will also affect the plant's carbon isotope ratios (Farquhar *et al*. 1982). Our understanding of the mechanism that causes changes on the carbon isotope imprint of plant biomass as a function of salinity is much greater than our understanding of the effects of salinity on the hydrogen (expressed as δ^2H values) and oxygen isotopic (expressed as $\delta^{18}O$ values) imprint in plant water and biomass.

Mangroves and other halophyte plants tend to discriminate against ^2H (deuterium) during water uptake and therefore the

hydrogen isotopic ratios of their stem water are more depleted relative to the source water (Lin and Sternberg 1995; Ellsworth and Williams 2007). This discrimination during water uptake only occurred in salt tolerant plants (Ellsworth and Williams 2007). It has been speculated that water must pass through the cell membrane during the ultrafiltration process and that this causes the observed discrimination. However, no evidence for this mechanism has been provided, other than the observation that there is discrimination during water movement through membranes of erythrocytes as an example (Karan and Macey 1980). Water in the leaves of mangroves and other halophyte plants also tends to be isotopically less enriched relative to stem water compared with those of freshwater plants (Romero and Feakins 2011; Ellsworth *et al*. 2013). In some cases, the closer the plant is associated with saline ocean water, the lower the isotopic enrichment of the leaf water (Romero and Feakins 2011). In the mangrove study by Ellsworth *et al*. (2013), differences in stem water isotope ratios between mangroves and freshwater plants were ruled out because leaf water isotope enrichment was expressed relative to that of stem water. We can also rule out the potential effect of differences in RH on leaf water isotopic enrichment between the seaward mangroves compared with that of the freshwater site. Sampling of mangrove and freshwater leaves were at most 30 m apart and measurements of RH at the two locations were not significantly different ($67.5 \pm 3.6\%$ for the freshwater site and $65.8 \pm 2.8\%$ for the mangrove site, $F = 1.74$, $P > 0.05$). This led us to the conclusion that there must be differences in water processing by leaves of mangroves compared with those of freshwater plants. Although many mangroves ultra-filtrate water during uptake, a considerable amount of salt in the xylem water still enters the leaf (Scholander *et al*. 1962). It has been speculated that as this water enters the leaf it must follow a different and longer desalinisation pathway to the stomatal cavity compared with xylem water entering the leaf of a freshwater plant (Ellsworth *et al*. 2013). This longer more extended pathway in the leaf of a halophyte plant could cause a lower leaf water isotopic enrichment. Leaf succulence is also inversely correlated with leaf water isotopic enrichment in mangroves compared with freshwater plants and could be contributing to this phenomenon (Ellsworth *et al*. 2013). However, other studies show no such correlation (Kahmen *et al*. 2009). Although no evidence has been forthcoming for this longer desalinisation pathway of water movement in mangrove leaves, there is a theoretical basis under the current leaf water isotopic enrichment model for leaf water being less enriched with a longer more tortuous pathway of water movement from the xylem to the stomatal cavity (Barbour and Farquhar 2004).

A factor that may also contribute to the lower leaf water isotopic enrichment in mangrove leaves is its stomata size and density. There are many studies showing the relationship between stomata size and density as a function of atmospheric CO_2 concentration (Woodward and Kelly 1995). A lower atmospheric CO_2 concentration is associated with smaller and more dense stomatal distribution of the leaf (Franks and Beerling 2009). It has been suggested that this relationship could be used with fossil leaves to estimate ancient atmospheric CO_2 concentration (Beerling and Royer 2002; Rundgren and Beerling 2003). Recently, the mechanism of how decrease in stomata size and increase in density allows for greater stomatal conductance and, therefore, greater CO_2 uptake in a CO_2 poor atmosphere has been elucidated (Franks and Beerling 2009). Conversely, larger stomata that are less densely distributed will lead to a lower leaf stomatal conductance. This same principle would apply for plants that need to minimise their water loss by transpiration under dry or saline conditions. Indeed, there are studies that show that plants which are bred for lower stomatal density and larger stomatal pores can better perform under saline conditions compared with those having higher stomatal density or smaller stomatal pores (Barbieri *et al*. 2012; Orsini *et al*. 2012). Concomitant with the changes in gas exchange brought about by the stomatal density and size, there are likely to be changes in the stomatal cavity volume and distribution in the entire leaf, which could certainly affect the isotopic enrichment of leaf water during transpiration. Here, using our own measurements for South Florida mangroves and freshwater plants together with those previously published, we first test the hypothesis that mangroves have larger less densely distributed stomatal pores than tropical freshwater plants. Second, using an artificial leaf model, we test the hypothesis that larger less dense pores lead to lower leaf water isotopic enrichment during evaporation than leaves having smaller more dense pores, even though the total pore area of these leaf models are similar. We then discuss how these observations may fit into the current leaf water isotopic enrichment model.

Materials and methods

Stomatal measurements

Samples collection sites

Leaf samples were obtained from several areas in the vicinity of Miami, Florida, including Fairchild Tropical Garden, The Kampong Garden, and the Gifford Arboretum at the University of Miami. The average annual rainfall for this region is 1480 mm. The mean temperature ranges from 30.4°C in the summer to 24.8°C in the winter months, and the annual mean RH is 83% (data from NOAA Climate Services, Miami, FL, 25.65°N, 80.30°W). Mangroves and transitional species (species frequenting the boarders of mangroves) were collected from damp environments in the vicinity of salt water at Fairchild Tropical Garden and at the Kampong Garden. Freshwater species and additional transitional species were collected on dry land at the University of Miami Gifford Arboretum and Fairchild Tropical Park.

Sample preparation and analysis

Leaves (3–4) were collected from an individual of each species and stored under refrigeration (5°C) for observation the next day. The leaves were carefully chosen for maturity and maximal sunlight exposure. They were removed at 4–5 nodes below the apex of the shoot. For analysis, small square sections were cut with a razor blade from the middle of the leaf avoiding the central vein. The surfaces were wiped clean and the sample squares placed in slides with the underside (abaxial side) of the leaf facing down. An image was prepared via high-resolution confocal microscope (Leica Microsystems Inc., Buffalo Grove, IL, USA), fluorescing the tissue with a helium neon laser at a wavelength of 458 nm, an optimal setting corresponding to the green chlorophyll of the plant. Stomata for each species were then

measured and counted using Fiji Image software (NIH, Bethesda, MD, USA), a program that calibrates each image in proportion to its actual area. Stomatal lengths and frequencies were measured by use of a drawing and charting tool featured by the above software. Three replicates were performed for each species. Each trial was performed on a different leaf, cutting a new square for observation in the same manner. In the case of *Conocarpus erectus* L. and *Laguncularia racemosa* (L.) C.F. Gaertn., stomata were also present on the top surface of the leaf. The top surfaces of each of the three specimens observed for these species were also imaged and averaged with bottom values, which were similar.

Statistical analysis

The R software was used to determine significant differences in stomatal size and frequency among species. An ANOVA test was performed to determine whether significant differences occurred between species, followed by Tukey's pairwise comparison test. We first performed statistical tests with our own measurements and then performed ANOVA between stomatal density and size of mangroves and its freshwater tropical counterpart species (tropical forest and savanna) with data pooled from the literature (Seshavatharam and Srivalli 1989; Bongers and Popma 1990; Li *et al*. 2009; Zhang and Cao 2009; Camargo and Marenco 2011; Zhang *et al*. 2012) and our measurement (excluding transitional species) to determine whether stomatal density and guard cell size of mangrove leaves differ from tropical freshwater species.

Artificial leaves

Artificial leaf components

To test how pore size and density affect leaf water isotopic enrichment ,we built simple artificial leaf models having pores of different sizes and densities, but similar total pore area. We chose an artificial leaf model rather than an assortment of different leaves having different stomatal densities because we do not exclude the possibility that other factors (such as pore area or vascularisation) can also affect isotope ratios of leaf water. The artificial models built here are identical in all aspects and only differ on pore size and density. The artificial leaves consisted of a top 104.4 cm^2 perforated 0.9 mm thick stainless steel plate having orifices of a specified diameter and acquired from OnlineMetals (Seattle, Washington DC, USA; Fig. 1). This top component simulates the epidermal tissue of the leaf with stomatal pores. A moist absorbent fibrous material underlies the top plate to simulate the leaf mesophyll (Whatman gel blotting paper, Grade GB2005, Sigma Aldrich, St Louis, MO, USA), followed by a 104.4 cm^2 plexiglas board that simulated leaf epidermal tissue without pores. We had two leaf versions, one with high pore density but smaller diameter (1.59 mm) and the other with lower pore density and larger diameter (3.19 mm). Specifications regarding the properties of each leaf model can be seen in Table 1. Because the factory made large pore diameter plates had an excess of pores, we randomly covered some of the pores with a hot glue gun to achieve a similar evaporative area as the small pore plate. At the beginning of the experiment the sandwiched components of the leaf model were sealed at the edges with electrical tape and allowed to evaporate under the turbulence of a small fan at laboratory conditions (average RH of 60% and average temperature of 22.0°C) for ~8 h. Model leaves were allowed to evaporate until ~50% of the water in the absorbent material evaporated off. At this point the artificial leaves were quickly disassembled and the absorbent material placed in a sealed tube for cryogenic distillation of the remaining water. Additionally, we sealed two moist absorbent sheets before any evaporation, to determine the initial isotopic composition of the artificial leaf water. The total initial amount of water in the middle layer was calculated by the difference in weight before and after wetting the absorbent material. By periodically weighing the leaf model starting at the beginning of the experiment we could

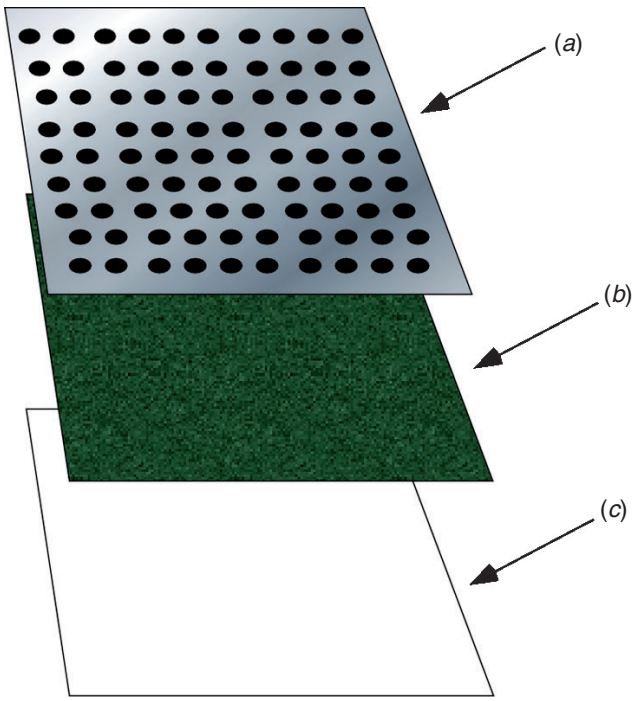

Fig. 1. Artificial leaf assembly: top layer (*a*) perforated stainless steel sheet, blotting paper saturated with water (*b*), and a lower layer of plexiglass (*c*). After assembly, layers were taped together at the edges with electrical tape and left to evaporate.

Table 1. Pore diameter, percent evaporative area relative to the total plate, pore density, total pore perimeter per plate and pore conductance for each artificial model leaf

Plate ID #	Pore diameter (mm)	Evaporative area (%)	Pore density cm^{-2}	Total perimeter of pores (cm)	Conductance (mol m^{-2} s^{-1})
1	3.19	22.5	2.8	22.3	0.11
2	3.19	21.8	2.7	21.6	0.10
3	3.19	21.3	2.7	21.1	0.10
4	1.59	21.8	11.0	43.4	0.15
5	1.59	21.8	11.0	43.4	0.15
6	1.59	21.8	11.0	43.4	0.15
7	3.19	21.5	2.7	21.3	0.10
8	1.59	21.8	11.0	43.4	0.15

keep track of how much water evaporated. Hence, we could calculate the fraction of water left in the artificial leaf after evaporation and the evaporation rate.

Isotopic analysis

Water from the absorbent material was cryogenically distilled as by Sternberg and Swart (1987). This extracted water was vaporised and analysed in a cavity ringdown spectrometer (Picarro Vaporisation module A0 211 and Picarro L2130-i Spectrometer, Santa Clara, CA, USA). Hydrogen and oxygen isotope ratios are expressed here as:

$$\delta^2\mathrm{H} \text{ or } \delta^{18}\mathrm{O} = \left(\frac{R_{sample}}{R_{std.}} - 1\right) \cdot 1000, \quad (1)$$

In which R_{sample} and R_{std} represent $^2H/^1H$ or $^{18}O/^{16}O$ of the sample and the standard for the calculation of δ^2H or $\delta^{18}O$ respectively. The standard used here is the Vienna provided Standard Mean Ocean Water (vSMOW). The precision of the analysis averaged 0.02‰ and 0.12‰ for oxygen and hydrogen isotope ratios respectively.

Data analysis

We tested for differences in the isotopic composition and other relevant parameters to leaf water isotopic enrichment after evaporation between the two types of leaves using a one-way ANOVA. We also tested for significant correlations and in some cases derived the best fit relationship between the isotopic composition of the tissue and different parameters attributed to each type of leaf model: total pore area, total perimeter of pore area, density of pore area, fraction of water remaining after evaporation and evaporation rate.

We considered several models potentially applicable to our artificial leaf system. Since, there is no external water input into the artificial leaves studied here, one might think that the model proposed by Helliker and Griffiths (2007) to interpret non-rooted epiphytes or that proposed by Hartard *et al*. (2009) to interpret lichens might be the most appropriate model. However, the Helliker and Griffiths (2007) model considers leaf water as a homogeneous well mixed body of water, which is clearly not the case here. Although the Hartard *et al*. (2009) model considers two mixing bodies of water in the lichen thallus, they do not consider stomatal pores, which is critical to our interpretation. Current models for leaf water isotopic enrichment assume input of stem water into the leaf or steady-state conditions (Barbour and Farquhar 2004; Farquhar and Cernusak 2005). For this reason, we took a different approach in analysing the data from the artificial leaves. Since the artificial leaves studied here had a finite quantity of water without any input from an external source, we considered that during transpiration the leaf water is undergoing an isotope Rayleigh distillation effect. The Rayleigh distillation equation predicts the isotope ratio of a limited pool of water without any external replenishment after a fractional withdrawal of water with a constant fractionation (Clark and Fritz 1997). Because our replicate leaves had different evaporation rates and had different fractions of water left when samples were collected, we were able fit it to the Raleigh equation. We only analysed oxygen isotope ratio of the artificial leaf water because only this isotope gave significant effects. We use here two expressions for fractionation α_{i-j}, which represents the heavy to light isotope ratios of one phase or compartment *i* of water over another *j* (R_i/R_j) and ε_{i-j}, which is $(\alpha_{i-j} - 1)1000$. First, we fitted the four replicates $\delta^{18}O$ values of each type of artificial leaf tissue to a Rayleigh distillation equation of the form:

$$\delta_{LW} = \delta_0 - \varepsilon_{LW-V} \ln(f), \quad (2)$$

where δ_{LW} and δ_o are the $\delta^{18}O$ values of the fraction of leaf water (f) remaining in the leaf after evaporation and the initial $\delta^{18}O$ value of the leaf water respectively, and ε_{LW-V} is the fractionation between the bulk leaf water and the vapour leaving the leaf. According to the Rayleigh equation, since the vapour leaving the leaf is isotopically depleted relative to bulk leaf water, there should be a progressive isotopic enrichment of the leaf water as the remaining fraction diminishes. We made no assumptions on the value of δ_o as it may have taken some time for ε_{LW-V} to reach a steady value and only fitted to the measured values of δ_{LW} and f. The slope of these regressions allowed us to estimate the fractionation factor between the bulk leaf water and the vapour leaving the leaf (ε_{LW-V}). Second, we used this value to calculate the $\delta^{18}O$ value of the vapour leaving each leaf by the following equation:

$$\delta_V = \delta_{LW} - \varepsilon_{LW-V}, \quad (3)$$

where δ_V is the isotope ratio of the vapour leaving each leaf. As a third step, we solved for the $\delta^{18}O$ value of the water at the evaporative surface underneath the pores generating this vapour (δ_{ev}) using Craig and Gordon's equation (Craig and Gordon 1965):

$$\delta_V = \frac{[\alpha_{eq}\delta_{ev} - h\delta_a - \varepsilon_{eq} - (1-h)\varepsilon_k]}{\left[(1-h) + \frac{(1-h)\varepsilon_k}{1000}\right]}, \quad (4)$$

where α_{eq}, ε_{eq} and ε_k are the different expressions for fractionation between vapour and liquid water due to equilibrium and kinetic processes respectively. The equilibrium fractionation is a function of temperature, and the kinetic fractionation is a function of pore and boundary layer conductance (Barbour and Farquhar 2004). We calculated these fractionation factors accordingly assuming that the temperature of the leaf and atmosphere were the same and 22°C, and the pore conductance was that given in Table 1 and the boundary layer conductance was assumed to be $1\,mol\,m^{-2}\,s^{-1}$. We used the average relative humidity of the laboratory (h) of 0.60 and the oxygen isotope ratio of ambient vapour (δ_a) commonly measured in the laboratory of –13‰. Forth, having both the $\delta^{18}O$ values of the bulk leaf water and that of the evaporative surface, we made the bold assumption that the Peclet effect applies to this non-steady-state situation and calculate a term that is only a function of the Peclet number ($\wp$) by the following equation (Barbour and Farquhar 2004):

$$\frac{1 - e^{-\wp}}{\wp} = \frac{\Delta_{LW}}{\Delta_{ev}}, \quad (5)$$

where Δ_{LW} and Δ_{ev} are the respective differences between δ_{LW} and δ_{ev} and the isotope ratio of the original water before evaporation (–1.1‰). Finally, using the above factor, the Peclet

number was then estimated by iteration and the effective path length water travels from the source to the evaporative surface (L) was calculated by using the Peclet equation:

$$\wp = \frac{E \cdot L}{D \cdot C}, \quad (6)$$

in which E (mol m^{-2} s^{-1}) is the evaporation rate relative to the artificial leaf surface, D (m^2 s^{-1}) is the diffusivity of water molecules containing the respective isotope through water and C (mol m^{-3}) is the molar density of water. The diffusivity D is a function of temperature (Cuntz *et al*. 2007) and was calculated accordingly at a temperature of 22°C.

Results

Stomatal pores in mangrove leaves measured here were less densely distributed and larger compared with freshwater plants growing nearby (Fig. 2*a*, *b*). There was a significant difference between stomatal density of local mangroves and freshwater

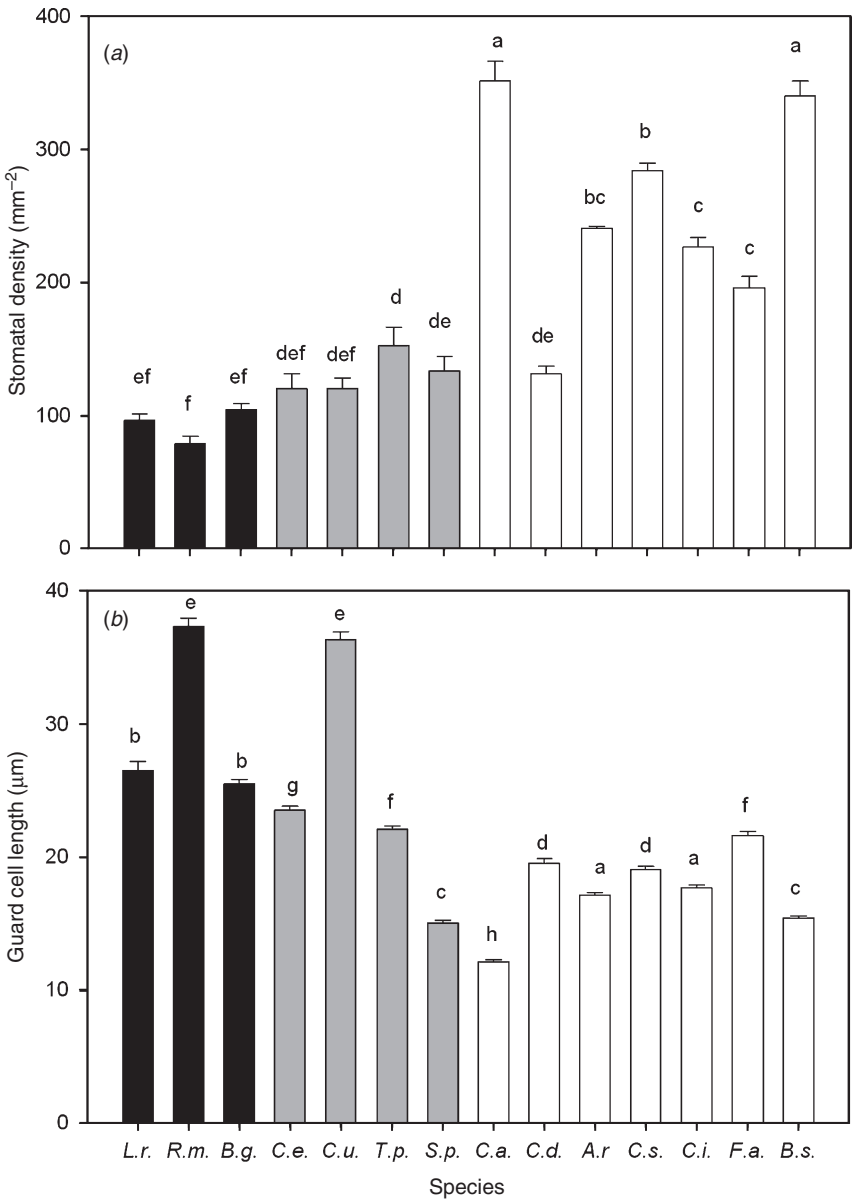

Fig. 2. Stomatal density (*a*) and guard cell length (*b*) of mangroves (black bars), transitional species (grey bars) and freshwater species (white bars). Bars not sharing a common letter have values that are significantly different than each other. Abbreviations for species are: *L.r. Laguncularia racemosa*, *R.m. Rhizophora mangle*, *B.g. Bruquiera gymnorrhiza*, *C.e., Conocarpus erecta*, *C.u. Coccoloba uvifera*, *T.p. Thespesia populnea*, *S.p. Scaevola plumerii*, *C.a. Calicarpa americana*, *C.d. Coccoloba diversifolia*, *A.r. Ardisia revoluta*, *C.s. Croton sylvaticus*, *C.i. Chrysobalanus icaco*, *F.a. Ficus aurea*; *B.s. Bursera simaruba*.

plants, with the exception of *Coccoloba diversifolia*. Although, the density of stomata for mangroves was lower than transitional species, mangroves only had significantly lower stomatal density compared with the transitional species *Thespesia populnea*. Guard cell length was significantly greater in mangroves than those of the local freshwater species. Guard cell length was significantly larger in mangroves compared with transitional species with exception of *Coccoloba uvifera*, which had similar pore sizes as *Rhizophora mangle*. A compilation of guard cell length (Gl) versus stomatal density (Sd) for our measurement of hardwood hammock species and those of several other studies of 134 freshwater tropical species (savannas and tropical forests) shows that there is a significant inverse relationship between these two variables ($Gl = 28.3e^{-0.0008 \times Sd}$, $r = 0.61$, $P < 0.01$); i.e. species with high stomatal density tended to have smaller guard cell length (Fig. 3). Average guard cell length (30 ± 1.7 µm, s.e.) of mangroves from our study and a compilation of other studies is significantly greater than those of freshwater tropical species (18.9 ± 0.6 µm, $F = 41.2$, $P < 0.01$, Fig. 3). In addition, mangrove average stomatal density of 187 ± 19 mm^{-2} was significantly lower ($F = 9$, $P < 0.01$) than the average stomatal density of 418 ± 28 mm^{-2} for freshwater species. Mangroves stomatal pore size and density not only seem to be exclusively found in the low density and large size end of the spectrum of values found in freshwater plants, they are larger than the freshwater plants for the range of stomatal densities observed in mangroves. The residual of mangroves pore size (observed pore size – predicted by the best fit relationship) at a range of density from 57 to 345 mm^{-2} (5.6 µm) is significantly greater ($F = 18.5$, $P < 0.05$) than the residuals observed for freshwater species found in this same range of densities (–1.8 µm).

Water from tissues of both types of artificial leaves became enriched in ^{18}O and ^{2}H relative to the source water. When these values were plotted in a δ^2H versus $\delta^{18}O$ plot, the data points fell in a line having a slope of 1.4, which intercepts the global meteoric water line at a δ^2H and $\delta^{18}O$ value of –17.7‰ and –3.5‰ respectively (Fig. 4*a*). The meteoric water and leaf water line intercept values are similar to the value of average rainfall in South Florida (Price *et al*. 2008). However, water from artificial leaves having smaller and denser pores became significantly more enriched in ^{18}O than those having larger and less dense pores ($F = 11.8$, $P = 0.01$, Fig. 4*a*, *b*). Although water from small pore and high-density artificial leaves was on average more enriched in ^{2}H compared with that of large pore and low-density model leaves, the difference was not significant ($F = 1.7$, $P = 0.23$, Fig. 4*b*). The $\delta^{18}O$ values of water from both types of artificial leaves after evaporation were not correlated with the total pore area ($r = 0.01$, $P > 0.05$), but correlated with total pore area perimeter ($r = 0.81$, $P < 0.05$) and density ($r = 0.81$, $P < 0.05$). There was a significant Rayleigh relationship between $\delta^{18}O$ values of water with the natural log of remaining fraction of water (large pore: $r = 0.97$, $P < 0.05$, small pore: $r = 0.95$, $P < 0.05$, Fig. 4*c*) and a significant polynomial relationship with evaporation rate (large pore: $r = 0.99$, $P < 0.01$, small pore: $r = 0.98$, $P < 0.05$, Fig. 4*d*) for each type of leaf considered separately. The δ^2H values of the artificial leaf water did not correlate with any of the above variables.

The slopes of the Rayleigh relationships (Eqn 2; Fig. 4*c*) show that there are differences in the fractionation between the isotope ratios of bulk leaf water and the vapour generated by transpiration for large pore/low density and small pore/high density leaves. The fractionation for the small pore/low density leaves was greater than those of the large pore/low density leaves (9.52 vs 4.63 respectively). The vapour generated by the large pore/low density leaves and the water at the evaporative surface was isotopically more enriched than that generated by the small pore/high density leaves and related to the evaporative rate for each leaf type (Fig. 5*a*, *b*). The Peclet ratio and effective path length was greater for large pore/low density leaves compared with those from small pore/high density leaves. Within each leaf type these parameters were also related to the evaporative rate and decreased as evaporation rates increased (Fig. 5*c*, *d*).

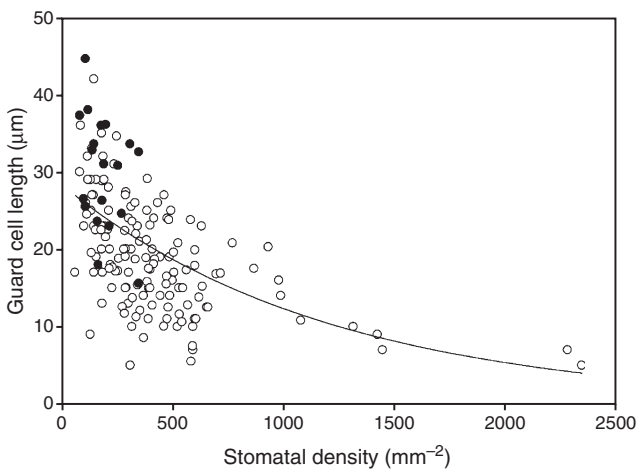

Fig. 3. Guard cell length (µm) versus stomatal density (mm^{-2}) for data from mangroves and freshwater plants collected in this study and data compiled from several studies. Black points represent values of mangrove species and clear points represent values of freshwater plants. Black line represents the best fit exponential decay fit to the values of the freshwater species ($y = 28.3e^{-0.0008x}$, $r = 0.61$, $P < 0.01$).

Discussion

Mangroves in South Florida tended to have fewer and larger stomatal pores compared with freshwater species. Transitional species occupying areas surrounding the mangroves, which may be exposed to occasional seawater, had stomatal densities and sizes intermediate to mangroves and freshwater species (Fig. 2*a*, *b*). In addition, a compilation of several mangroves species, (14) including those growing in India and China, all seem to show the same trend with mangroves occupying one of extremities of the size/density spectrum found for 134 freshwater plant species reported in the literature (Fig. 3). Recently it has been elucidated that the often observed higher stomatal density and smaller stomatal size, observed when plants are exposed to low ambient CO_2 concentration, allows for a greater maximum stomatal conductance (Franks and Beerling 2009). This greater stomatal conductance allows the plant to more efficiently absorb CO_2 during periods where its concentration is low. In contrast, geological periods of high CO_2 concentration typically have leaves with larger and less dense stomatal pores (Rundgren and Beerling 2003; Franks and Beerling 2009; Doria *et al*. 2011). This allows for greater conservation of water during gas exchange

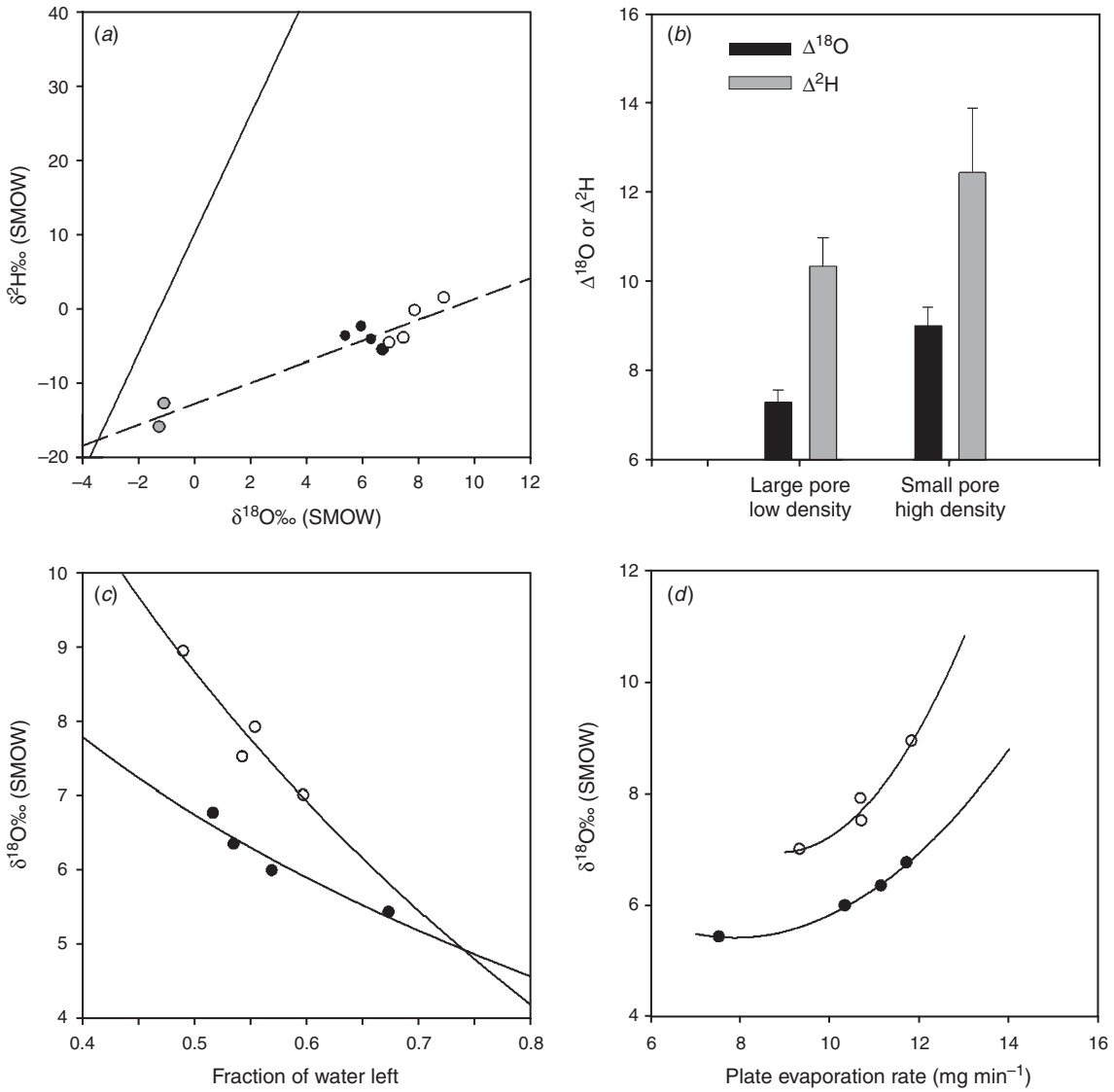

Fig. 4. Isotope ratios of artificial leaves after evaporation. (*a*) Hydrogen versus oxygen isotope ratios of source water (grey points), leaves with large low density pores (●) and small high density pores (○). Dashed lines represent the best-fit relationship for all points having a slope of 1.4. Solid line represents values expected for the meteoric water line ($\delta^2H = (8\delta^{18}O) + 10$). (*b*) Leaf water isotopic enrichment relative to the source water for large pore low-density artificial leaves and small pore high density leaves. (*c*) The relationship between $\delta^{18}O$ values of leaf water versus the fraction remaining after evaporation (*f*). For large pore low density leaves: $\delta^{18}O = 3.54–4.63\ \mathrm{Ln}(f)$, $r = 0.96$, $P < 0.05$. For small pore high density leaves: $\delta^{18}O = 2.07–9.52\ \mathrm{Ln}(f)$, $r = 0.95$, $P < 0.05$. (*d*) The relationship between $\delta^{18}O$ values of bulk leaf water versus the evaporation rate (*E*). For large pore low density leaves: $\delta^{18}O = 0.09E^2 - 1.42E + 11.01$, $r = 1.0$, $P < 0.05$. For small pore high density leaves: $\delta^{18}O = 0.23E^2 - 4.12E + 25.31$, $r = 0.98$, $P < 0.05$.

by the leaf. The critical aspect causing the modulation of stomatal conductance of leaves as a function of size and density is the observation that the path length through which gases have to pass through during leaf gas exchange increases with guard cell size (Franks and Farquhar 2007). Thus, two leaves with similar total pore area, but one having larger and less dense pores will experience a lower maximum stomatal conductance as the path length that gases have to pass through are longer for the larger pore leaf. We speculate that the larger and less dense stomatal pore found in mangroves is a water conserving strategy for these halophyte plants.

The water conserving strategy mentioned above probably imprints on the oxygen and hydrogen isotope ratio of leaf water and mangrove biomass. We have observed in South Florida that mangrove leaf water is not as ^{18}O enriched as freshwater plants, which tend to have leaves with smaller pores and higher density (Ellsworth *et al*. 2013). This was observed despite both mangrove and freshwater plants being exposed to similar relative humidity. This lower leaf water isotopic enrichment is propagated on to oxygen isotope ratios of cellulose synthesised in mangrove stems. Oxygen isotope ratios of stem cellulose from mangroves do not reflect the

oxygen isotope ratios of the isotopically enriched seawater they are exposed to (Ellsworth *et al*. 2013). Others (Verheyden *et al*. 2004) have observed the same lack of expected oxygen isotopic enrichment in biomass of mangroves, although these authors did not measure the oxygen isotope ratios of leaf water directly. The same phenomenon of lower than expected enrichment has also been observed in the hydrogen isotope ratios of alkenes in mangroves and other halophytic plants (Romero and Feakins 2011; Nemiah Ladd and Sachs 2012). One of these studies (Romero and Feakins 2011) sampled leaf water and also observed that the isotopic enrichment of leaf water decreases with proximity to the ocean.

As predicted, we observed that artificial leaves with smaller and more densely distributed pores, which would be equivalent to freshwater species, had water with $\delta^{18}O$ values significantly greater then water from artificial leaves having the larger and less dense pores, which would be the equivalent of mangrove leaves (Fig. 4). This difference in isotopic enrichment occurred even though both types of artificial leaves had similar total evaporative area (Table 1). There was a weaker hydrogen isotope ratio response to pore size and density in the artificial leaf water. In general, leaf water undergoing evaporation will have $\delta^{18}O$ and $\delta^{2}H$ values such that values of $\delta^{2}H$ vs $\delta^{18}O$ plot in a line with a slope much less than that observed for the meteoric water line (8) and averaging 2 or 3 (Fig. 4*a*) (Allison *et al*. 1985). The lower slope is the effect of the kinetic isotope fractionations that affects the oxygen isotope ratio of evaporative water to a similar extent as the hydrogen isotope ratios, causing the slope to approach unity.

Our dissection of the various components that lead to differences in the oxygen isotopic enrichment between water from large pore/low density and small pore/high density leaves (Fig. 5), not only informs us on the causes of the isotopic differences due to pore size and density, but also dispels some implicit assumptions regarding the processes which lead to leaf water isotopic enrichment in real leaves. We will first discuss the causes for differences between leaves having different pore size and density followed by a discussion on how the artificial leaf experiments shown here relate to studies on isotope ratio of water in real leaves.

Our explanation regarding the causes for the differences in the isotope ratios of water between large pore/low density and small pore/high density leaves is based on our assumption that the Peclet effect is important to the isotopic enrichment of the artificial leaf water as in Eqn 5. If our assumption is correct,

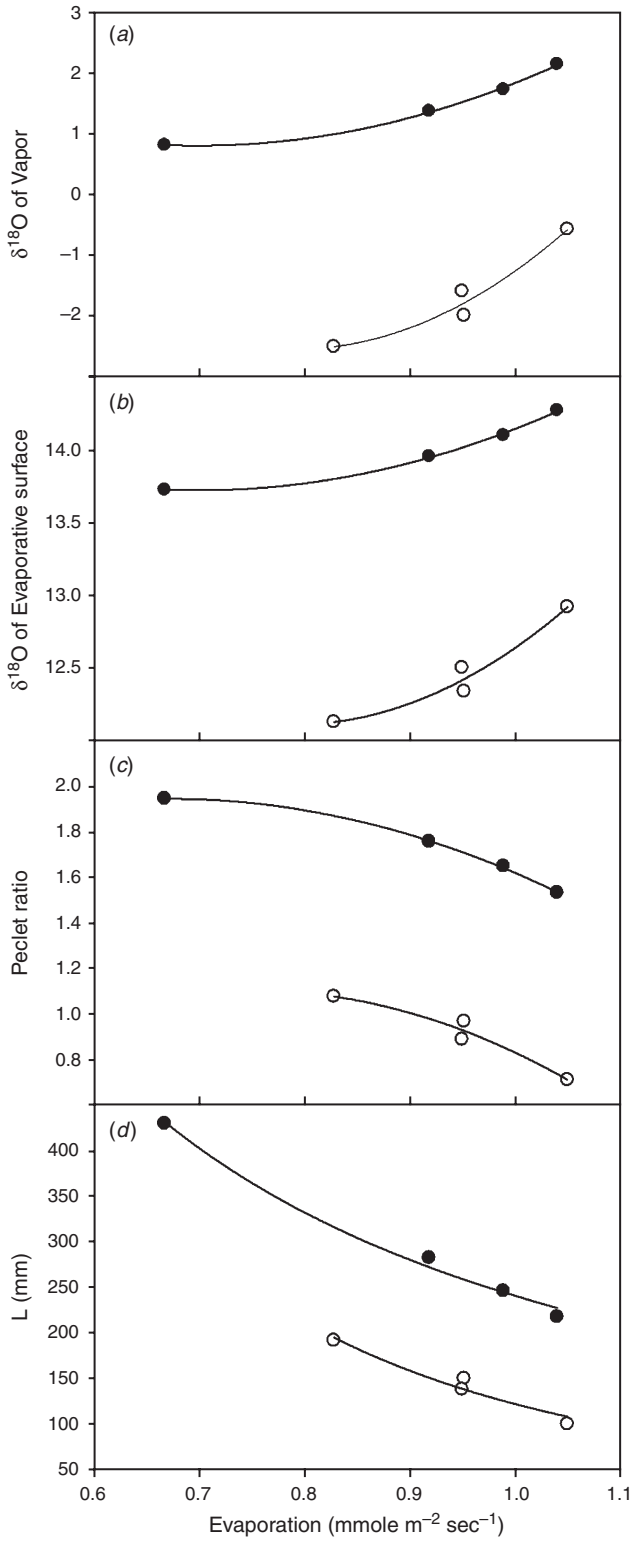

Fig. 5. Oxygen isotope ratios of vapour lost by artificial leaves (*a*) and of the evaporative surface generating the vapour (*b*) as a function of evaporation rate (mmol m^{-2} s^{-1}). Also shown are the Peclet ratio (*c*) and effective path length water travels to the evaporative surface (*d*) as a function of evaporation rate. Symbols are ● for large pore/low density leaves and ○ for small pore/high density leaves. The best fit regression lines are for isotope ratios of vapour as a function of evaporation are described by: $\delta_V = 6.4 - 16.0E + 11.4E^2$, $r = 0.999$, $P < 0.01$ and $\delta_V = 15.8 - 46.4E + 29.4E^2$, $r = 0.978$, $P < 0.01$ for large pore/low density and small pore/high density leaves respectively. Regression lines for the isotope ratios of the evaporative surface generating the vapour are: $\delta_{ev} = 16.0 - 6.5E + 4.7\,E^2$, $r = 0.999$, $P < 0.01$ and $\delta_{ev} = 19.6 - 19_E + 12.0E^2$, $r = 0.978$, $P < 0.01$ for large pore/low density and small pore/high density leaves respectively. Regression lines for the Peclet effect as a function of evaporation rate are: $\wp = 0.6 + 4.0E + 3.0E + 3.0E^2$, $r = 0.999$, $P < 0.01$ and $\wp = -1.4 + 6.6E + 4.4E^2$, $r = 0.976$, $P < 0.01$ for large pore/low density and small pore/high density leaves respectively. Regression lines for the effective path length and evaporation rates are: $L = 240.5E^{-1.45}$, $r = 0.996$, $P < 0.01$ and $L = 122.0E^{-2.5}$, $r = 0.974$, $P < 0.1$ for large pore/low density and small pore/high density leaves respectively.

then the higher Peclet number for large pore/low-density leaves causes their bulk water to have a lower isotopic enrichment than those of small pore/high density leaves (Fig. 5*c*; Eqn 5). A further understanding of the components of the Peclet ratio is necessary to fully understand how pore size can affect the Peclet ratio. In addition to the evaporation rate, diffusivity and the molar volume of water determining the Peclet ratio, another important component is the effective distance over which the advective flux is occurring (Eqn 6). The original calculation of the Peclet ratio assumes that advection of water is occurring across a symmetrical slab, which is far from the complex structure of a leaf. For example: evaporation relative to the leaf surface area or the leaf thickness does not fully express the cross-sectional area and true length water has to travel through the mesophyll. Water can travel through many pathways having different cross-sectional areas as it moves from the xylem to the stomatal cavity and it does not move in a straight line. The expression of advective flow as the vapour moving across the leaf surface area simplifies the fact that advective flow occurs with liquid water along the complex topography of the mesophyll. For this reason the effective path length (L) is a correction for this over-simplification by multiplying two factors (*k* and *l*): a scalar *k*, which is the ratio of leaf surface area to the total cross-sectional area perpendicular to the path of advective flow; and *l*, the true length of the pathway from the xylem to the stomatal cavity in metres (Cernusak and Kahmen 2013). We propose here that the variation in stomatal size and density and its associated stomatal cavities directly impact on both components (*k* and *l*) of L in the Peclet ratio.

With this knowledge of the components of the Peclet ratio we can determine why larger/less densely distributed pores in a leaf will cause the Peclet ratio to increase. When both large pore/low density and small pore/high density leaf models are considered together, their water oxygen isotopic ratios were not related to the total pore area of the leaf, but were significantly related to density and the total pore perimeter. These two factors could affect the Peclet ratio and thus modulate artificial leaf water isotopic enrichment. Although the artificial leaves here had no xylem water, one could consider that path length for the artificial leaves is the path length l of water movement from non-evaporating sites having isotopically non-enriched water to the site of evaporation. It is clear that a less dense pore distribution would cause an increase in this path length. In the artificial or real leaves, a less dense pore distribution would increase path length, increasing the Peclet number, which would diminish the isotopic enrichment of the leaf water. For this to be true in a real leaf, one would have to assume that leaf venation does not scale to pore density to maintain a constant l, regardless of density. The other Peclet component affected by the pore perimeter is the cross-sectional area perpendicular to the advective flow relative to the leaf surface area (*k*). Consider two leaves with the same evaporative loss and stomatal pore area, but differing in stomatal density and size, such that one leaf has high stomatal density but smaller stomata compared with the other. If the stomatal cavity volume scales to pore area then both leaves will have the same total stomatal cavity volume, but their individual stomatal cavities will have different surface area to volume ratios. Because the surface area to volume ratio decreases with an increase in volume, one expects the larger/lower pore density leaf to have a lower total stomatal cavity surface area – equivalent to a lower perimeter in our large pore artificial leaf. Ultimately this would decrease the cross-sectional area perpendicular to advective flow, increase k and the Peclet ratio. Hence, a total lower stomatal cavity surface area, such as that found in leaves having low density of large stomatal pores, would drive the Peclet ratio up and decrease the leaf water isotopic enrichment relative to small/higher density pore leaves having a higher stomatal cavity surface area.

There were unexpected observations of the different components contributing to the isotopic enrichment of leaf water (Fig. 5). The observation that the isotope ratio of the vapour lost by the less isotopically enriched large pore/low density leaves is greater than that from the more enriched small pore/high density leaves is logical by mass balance principles (Fig. 5*a*). In other words, given two leaves having the same water budget (same evaporation and influx of stem water), the one having bulk water isotopically more depleted than the other will, by mass balance principles, lose vapour that is isotopically more enriched compared with the other one. But what was unexpected and perhaps counter intuitive is that water at the site of evaporation will be isotopically more enriched for the leaf with a lower bulk water isotopic enrichment (Fig. 5*b*). The current steady-state leaf model assumes that the isotopic composition of water at the evaporative site is constant and only a function of the isotope ratio of atmospheric vapour and stem water. We show here that the pore size has an effect on the oxygen isotope ratio of the water at the evaporative site. It is possible that the higher advective flux rate in the large pore/low density leaves actually concentrates any isotopically enriched water that diffused away from the evaporative site back to the evaporative site. This would maintain the evaporative site more enriched while lowering the isotope ratio of the bulk leaf water. We note that the non-steady-state model of leaf water enrichment allows for the Peclet effect to influence the isotopic composition of the evaporative site (Farquhar and Cernusak 2005). The other surprising observation is that there is a change in the effective path length (L) with evaporation rate (Fig. 5*d*), which subsequently affects the Peclet ratio and the isotopic composition of the evaporative site and vapour. The decrease in effective path length with an increase in evaporation rate in our artificial leaves is similar to the observations of Song *et al*. (2013) and Ferrio *et al*. (2012) who observed the same trend in several tree species. Our range of L (100–400 mm) for evaporation rates ranging from 0.6 to 1.1 mmol m^{-2} s^{-1} are similar to those observed by Song *et al*. (2013) in real leaves. Song *et al*. (2013) speculated that shifts in advective flux between apoplastic, aquaporine and plasmodesmata pathways with changes in evaporation rate might be contributing to the inverse relationship between L and evaporation rate. However, since we were able to reproduce their phenomenon in a relatively amorphous cellulosic material, it suggests that this property may be more basic to water movement in a porous media. Perhaps high evaporation rates desiccate cellulosic fibres to some extent, lowering the hydraulic conductance and only allowing for water transport over a shorter distance. Alternatively, it could be that higher transpiration is only sustained when large cross-sectional area channels are available for advective flow. This would lower *k* and decrease the Peclet ratio.

The findings reported here have implications in the application of oxygen stable isotope abundance of tree rings to interpret climate change and ecological processes. Atmospheric CO_2 concentration has been increasing (Manning *et al*. 2011). Further, warmer geological periods are associated with higher CO_2 concentrations (Doria *et al*. 2011). Concomitant with the climate change associated with the increase in this greenhouse gas, plants will decrease their stomatal density and compensate it with larger stomatal pores (Rundgren and Beerling 2003; Doria *et al*. 2011). This decrease in stomatal density, as we have shown here, contributes to a lower leaf water isotopic enrichment that should pass on to lower enrichment of the oxygen isotope values of cellulose. Therefore, we would expect a stomatal density and size signal superimposed in the cellulose isotopic climate signal of a warming trend. Previously published results from tree ring oxygen isotope ratios of Metasequoia cellulose from Eocene fossils (Jahren and Sternberg 2002; Richter *et al*. 2008) exemplifies the above scenario. It has been shown that the stomatal density is low during this period as a response to CO_2 concentrations as high as 1000 µmol mol^{-1} (Doria *et al*. 2011). One would expect that along with this warmer period, rainfall and available water for plant growth would be somewhat more enriched compared with that presently observed in this Arctic location (Dansgaard 1964) and that this would pass on to the plant cellulose oxygen isotope ratio (Jahren and Sternberg 2002; Richter *et al*. 2008). However, analysis of fossil cellulose shows a greater depletion than expected when compared with modern day samples. According to our findings here, this lower than expected isotopic value of cellulose could be caused by low leaf water enrichment due to low stomatal density as a response to high atmospheric CO_2 concentration. Our observations might also explain why there is such a high species dependent variability in leaf water isotopic enrichment (Wang *et al*. 1998). There is high variability in stomatal density even for species growing in the same community. For example, stomatal density ranges from 179 to 1076 mm^{-2} in a Chinese savanna. This high stomatal density variability could cause differences in leaf water isotopic enrichment. Finally, leaf water has an impact in the oxygen isotope ratios of atmospheric CO_2 and O_2. The isotopic identity of these gases can be sensitive indicators of global processes (Farquhar *et al*. 1993; Beerling 1999). The stomatal density response of plants to the environment and its effect on the oxygen isotope ratios of leaf water would certainly provide feedback loops that could either dampen or amplify the isotopic signal from these gases.

References

Allison GB, Gat JR, Leaney FWJ (1985) The relationship between deuterium and oxygen-18 delta values in leaf water. *Chemical Geology* **58**, 145–156. doi:10.1016/0168-9622(85)90035-1

Barbieri G, Vallone S, Orsini F, Paradiso R, De Pascale S, Negre-Zakharov F, Maggio A (2012) Stomatal density and metabolic determinants mediate salt stress adaptation and water use efficiency in basil (*Ocimum basilicum* L.). *Journal of Plant Physiology* **169**, 1737–1746. doi:10.1016/j.jplph.2012.07.001

Barbour MM, Farquhar GD (2004) Do pathways of water movement and leaf anatomical dimensions allow development of gradients in $H_2{}^{18}O$ between veins and the sites of evaporation within leaves? *Plant, Cell & Environment* **27**, 107–121. doi:10.1046/j.0016-8025.2003.01132.x

Beerling DJ (1999) The influence of vegetation activity on the Dole effect and its implications for changes in biospheric productivity in the mid-Holocene. *Proceedings of the Royal Society of London. Series B, Biological Sciences* **266**, 627–632. doi:10.1098/rspb.1999.0682

Beerling DJ, Royer DL (2002) Reading a CO_2 signal from fossil stomata. *New Phytologist* **153**, 387–397. doi:10.1046/j.0028-646X.2001.00335.x

Bongers F, Popma J (1990) Leaf characteristics of the tropical rain-forest flora of Los-Tuxtlas, Mexico. *Botanical Gazette* **151**, 354–365. doi:10.1086/337836

Camargo MAB, Marenco RA (2011) Density, size and distribution of stomata in 35 rainforest tree species in Central Amazonia. *Acta Amazonica* **41**, 205–212. doi:10.1590/S0044-59672011000200004

Cernusak LA, Kahmen A (2013) The multifaceted relationship between leaf water ^{18}O enrichment and transpiration rate. *Plant, Cell & Environment* **36**, 1239–1241. doi:10.1111/pce.12081

Clark ID, Fritz P (1997) 'Environmental isotopes in hydrology.' (Lewis Publishers: New York)

Colmer TD, Flowers TJ (2008) Flooding tolerance in halophytes. *New Phytologist* **179**, 964–974. doi:10.1111/j.1469-8137.2008.02483.x

Craig H, Gordon LI (1965) Deuterium and oxygen-18 variations in the ocean and marine atmosphere. In 'Proceedings of the conference on stable isotopes in oceanographic studies and paleotemperatures'. (Ed. E Tongiorgi) pp. 9–130. (Laboratory of Geology and Nuclear Science: Piza)

Cuntz M, Ogee J, Farquhar GD, Peylin P, Cernusak LA (2007) Modelling advection and diffusion of water isotopologues in leaves. *Plant, Cell & Environment* **30**, 892–909. doi:10.1111/j.1365-3040.2007.01676.x

Dansgaard W (1964) Stable isotopes in precipitation. *Tellus* **16**, 436–468. doi:10.1111/j.2153-3490.1964.tb00181.x

Doria G, Royer DL, Wolfe AP, Fox A, Westgate JA, Beerling DJ (2011) Declining atmospheric CO_2 during the late middle Eocene climate transition. *American Journal of Science* **311**, 63–75. doi:10.2475/01.2011.03

Ellsworth PZ, Williams DG (2007) Hydrogen isotope fractionation during water uptake by woody xerophytes. *Plant and Soil* **291**, 93–107. doi:10.1007/s11104-006-9177-1

Ellsworth PV, Ellsworth PZ, Anderson WT, Sternberg LSL (2013) The role of effective leaf mixing length in the relationship between the $\delta^{18}O$ of stem cellulose and source water across a salinity gradient. *Plant, Cell & Environment* **36**, 138–148. doi:10.1111/j.1365-3040.2012.02562.x

Farquhar GD, Cernusak LA (2005) On the isotopic composition of leaf water in the non-steady state. *Functional Plant Biology* **32**, 293–303. doi:10.1071/FP04232

Farquhar GD, Ball MC, von Caemmerer S, Roksandic Z (1982) Effect of salinity and humidity on $\delta^{13}C$ value of halophytes- evidence for diffusional isotope fractionation determined by the ratio of intercellular/atmospheric partial pressure of CO_2 under different environmental conditions. *Oecologia* **52**, 121–124. doi:10.1007/BF00349020

Farquhar GD, Lloyd J, Taylor JA, Flanagan LB, Syvertsen JP, Hubick KT, Wong SC, Ehleringer JR (1993) Vegetation effects on the isotope composition of oxygen in atmospheric CO_2. *Nature* **363**, 439–443. doi:10.1038/363439a0

Ferrio JP, Pou A, Florez-Sarasa I, Gessler A, Kodama N, Flexas J, Ribas-Carbo M (2012) The Peclet effect on leaf water enrichment correlates with leaf hydraulic conductance and mesophyll conductance for CO_2. *Plant, Cell & Environment* **35**, 611–625. doi:10.1111/j.1365-3040.2011.02440.x

Flowers TJ, Colmer TD (2008) Salinity tolerance in halophytes. *New Phytologist* **179**, 945–963. doi:10.1111/j.1469-8137.2008.02531.x

Flowers TJ, Troke PF, Yeo AR (1977) Mechanism of salt tolerance in halophytes. *Annual Review of Plant Physiology and Plant Molecular Biology* **28**, 89–121. doi:10.1146/annurev.pp.28.060177.000513

Franks PJ, Beerling DJ (2009) Maximum leaf conductance driven by CO_2 effects on stomatal size and density over geologic time. *Proceedings of the National Academy of Sciences of the United States of America* **106**, 10343–10347. doi:10.1073/pnas.0904209106

Franks PJ, Farquhar GD (2007) The mechanical diversity of stomata and its significance in gas-exchange control. *Plant Physiology* **143**, 78–87. doi:10.1104/pp.106.089367

Hartard B, Cuntz M, Maguas C, Lakatos M (2009) Water isotopes in desiccating lichens. *Planta* **231**, 179–193. doi:10.1007/s00425-009-1038-8

Helliker BR, Griffiths H (2007) Toward a plant-based proxy for the isotope ratio of atmospheric water vapor. *Global Change Biology* **13**, 723–733. doi:10.1111/j.1365-2486.2007.01325.x

Jahren AH, Sternberg L (2002) Eocene meridional weather patterns reflected in the oxygen isotopes of Arctic fossil wood. *GSA Today* **12**, 4–9. doi:10.1130/1052-5173(2002)012<0004:EMWPRI>2.0.CO;2

Kahmen A, Simonin K, Tu K, Goldsmith GR, Dawson TE (2009) The influence of species and growing conditions on the ^{18}O enrichment of leaf water and its impact on 'effective path length'. *New Phytologist* **184**, 619–630. doi:10.1111/j.1469-8137.2009.03008.x

Karan DM, Macey RI (1980) The permeability of the human red-cell to deuterium oxide (heavy-water). *Journal of Cellular Physiology* **104**, 209–214. doi:10.1002/jcp.1041040210

Krauss KW, Ball MC (2013) On the halophytic nature of mangroves. *Trees – Structure and Function* **27**, 7–11. doi:10.1007/s00468-012-0767-7

Li Y, Li Z, Lin P, Soc IC (2009) The study on the leaf anatomy of some mangrove species of CHINA. In 'Proceedings of the 2009 International Conference on Environmental Science and Information Application Technology, Vol. III'. pp. 47–51. (Ieee Computer Society: Los Alamitos, CA, USA)

Lin G, Sternberg LdSL (1995) Hydrogen isotopic fractionation by plant roots during water uptake in coastal wetland plants. In 'Perspective on carbon and water relations from stable isotopes'. (Eds J Ehleringer, G Farquhar, A Hall) pp. 497–510. (Academic Press: New York)

Manning AC, Nisbet EG, Keeling RF, Liss PS (2011) Greenhouse gases in the earth system: setting the agenda to 2030. *Philosophical Transactions. Series A, Mathematical, Physical, and Engineering Sciences* **369**, 1885–1890. doi:10.1098/rsta.2011.0076

Nemiah Ladd SN, Sachs JP (2012) Inverse relationship between salinity and n-alkane δD values in the mangrove *Avicennia marina*. *Organic Geochemistry* **48**, 25–36. doi:10.1016/j.orggeochem.2012.04.009

Orsini F, Alnayef M, Bona S, Maggio A, Gianquinto G (2012) Low stomatal density and reduced transpiration facilitate strawberry adaptation to salinity. *Environmental and Experimental Botany* **81**, 1–10. doi:10.1016/j.envexpbot.2012.02.005

Price RM, Swart PK, Willoughby HE (2008) Seasonal and spatial variation in the stable isotopic composition ($\delta^{18}O$ and δD) of precipitation in south Florida. *Journal of Hydrology* **358**, 193–205. doi:10.1016/j.jhydrol.2008.06.003

Richter SL, Johnson AH, Dranoff MM, LePage BA, Williams CJ (2008) Oxygen isotope ratios in fossil wood cellulose: isotopic composition of Eocene- to Holocene-aged cellulose. *Geochimica et Cosmochimica Acta* **72**, 2744–2753. doi:10.1016/j.gca.2008.01.031

Romero IC, Feakins SJ (2011) Spatial gradients in plant leaf wax D/H across a coastal salt marsh in southern California. *Organic Geochemistry* **42**, 618–629. doi:10.1016/j.orggeochem.2011.04.001

Rundgren M, Beerling D (2003) Fossil leaves: effective bioindicators of ancient CO_2 levels? *Geochemistry Geophysics Geosystems* **4**, 1058. doi:10.1029/2002GC000463

Scholander PF (1968) How mangroves desalinate seawater. *Physiologia Plantarum* **21**, 251–261. doi:10.1111/j.1399-3054.1968.tb07248.x

Scholander PF, Hemmingsen E, Garey W, Hammel HT (1962) Salt balance in mangroves. *Plant Physiology* **37**, 722–729. doi:10.1104/pp.37.6.722

Seshavatharam V, Srivalli M (1989) Systematic leaf anatomy of some Indian mangroves. *Proceedings of the Indian Academy of Sciences-Plant Sciences* **99**, 557–565.

Song X, Barbour MM, Farquhar GD, Vann DR, Helliker BR (2013) Transpiration rate relates to within- and across-species variations in effective path length in a leaf water model of oxygen isotope enrichment. *Plant, Cell & Environment* **36**, 1338–1351. doi:10.1111/pce.12063

Sternberg L, Swart PK (1987) Utilization of freshwater and ocean water by costal plants of Southern Florida. *Ecology* **68**, 1898–1905. doi:10.2307/1939881

Verheyden A, Helle G, Schleser GH, Dehairs F, Beeckman H, Koedam N (2004) Annual cyclicity in high-resolution stable carbon and oxygen isotope ratios in the wood of the mangrove tree *Rhizophora mucronata*. *Plant, Cell & Environment* **27**, 1525–1536. doi:10.1111/j.1365-3040.2004.01258.x

Wang XF, Yakir D, Avishai M (1998) Non-climatic variations in the oxygen isotopic compositions of plants. *Global Change Biology* **4**, 835–849. doi:10.1046/j.1365-2486.1998.00197.x

Winter K, Holtum JAM (2005) The effects of salinity, crassulacean acid metabolism and plant age on the carbon isotope composition of *Mesembryanthemum crystallinum* L., a halophytic C_3-CAM species. *Planta* **222**, 201–209. doi:10.1007/s00425-005-1516-6

Woodward FI, Kelly CK (1995) The influence of CO_2 concentration on stomatal density. *New Phytologist* **131**, 311–327. doi:10.1111/j.1469-8137.1995.tb03067.x

Zhang JL, Cao KF (2009) Stem hydraulics mediates leaf water status, carbon gain, nutrient use efficiencies and plant growth rates across dipterocarp species. *Functional Ecology* **23**, 658–667. doi:10.1111/j.1365-2435.2009.01552.x

Zhang JL, Poorter L, Cao KF (2012) Productive leaf functional traits of Chinese savanna species. *Plant Ecology* **213**, 1449–1460. doi:10.1007/s11258-012-0103-8